

Magneto-optical properties of the competing-anisotropy model system $\text{Fe}_{1-x}\text{Co}_x\text{Cl}_2$. II. Faraday rotation

W. Nitsche and W. Kleemann

Laboratorium für Angewandte Physik, Universität Duisburg, Postfach 10 16 29, D-4100 Duisburg 1, Federal Republic of Germany

(Received 17 July 1987; revised manuscript received 14 December 1987)

The uniform magnetization, M , of the mixed antiferromagnetic system $\text{Fe}_{1-x}\text{Co}_x\text{Cl}_2$ is measured via the Faraday rotation θ at $\lambda=633$ nm in axial magnetic fields, $H \lesssim 25$ kOe, at temperatures 3.5 K $< T < 30$ K. By utilizing distinct changes of one or two of the functions (θ , $d\theta/dT$, or $d\theta/dH$) versus T or H arising at phase boundaries, the H -versus- T phase diagrams are constructed. For the easy-direction configurations $x=0.20$ and 0.27 , metamagnetic behavior with a tricritical point (13.93 K, 8.3 kOe) and spin-flop behavior with a bicritical point (14.60 K, 1.5 kOe), respectively, is found in accordance with predictions of Galam and Aharony. In addition, the spin-flip phase ($x=0.20$) is clearly indicated by transparent magnetic circular dichroism. For the easy-plane configurations, $x=0.315$ and 0.70 , single phase lines emerge. In the low-field limit, random-field Ising-model behavior is found for both $x=0.20$ and 0.27 as predicted by Fishman and Aharony. The crossover and specific-heat exponents, $\phi \sim 1.40$ and $\bar{\alpha} \sim 0$, respectively, disagree with previous results of Wong *et al.*, but confirm theoretical predictions in accordance with results on diluted antiferromagnets. Enhanced magnetization due to random-field-induced domain states appears upon crossing the phase boundaries paramagnetic (or spin-flop) -to-antiferromagnetic from high temperatures (fields) at H (T)=const, respectively. Domain states due to random intraplanar spin anisotropy are believed to appear at the smeared paramagnetic-to-spin-flop transition for $x=0.27$.

I. INTRODUCTION

In the last few years much interest has been focused onto the concentration (x)-versus-temperature (T) phase diagram of the competing-anisotropy model system $\text{Fe}_{1-x}\text{Co}_x\text{Cl}_2$.¹ It describes antiferromagnetic (AF)-to-paramagnetic (PM) upper phase transitions (PT) occurring at T_{c1} , and AF-to-oblique antiferromagnetic (OAF) PT's occurring at T_{c2} . All phase lines meet in a tetracritical point ($x_t \approx 0.28$), as depicted in Fig. 1. Some experimental investigations²⁻⁵ have also been done on the magnetic field dependence of the phase diagram. They were stimulated by the theoretical work of Fishman and Aharony⁶ (FA) and Galam and Aharony (GA),⁷ who predicted interesting new features of critical and multicritical behavior, respectively.

FA (Ref. 6) proposed that $\text{Fe}_{1-x}\text{Co}_x\text{Cl}_2$, when exposed to relatively weak longitudinal magnetic fields, H , would be a suitable system for studying three-dimensional (3D) random-field Ising model (RFIM) behavior. They generally showed that a random-exchange Ising model (REIM) antiferromagnet in a uniform external field is equivalent to an Ising ferromagnet in a random field (RF), which was originally treated by Imry and Ma.⁸ This equivalence should apply to $\text{Fe}_{1-x}\text{Co}_x\text{Cl}_2$ in the range $0 < x < x_t$, where Ising anisotropy prevails and S_{\parallel} ordering occurs at T_{c1} . It should be noticed that this prediction attracted much less attention than that concerning diluted Ising antiferromagnets like $\text{Fe}_{1-x}\text{Zn}_x\text{F}_2$. These are expected to behave similarly⁶ and have been considered to be the most perfect realizations of the RFIM up to now.⁹

The 3D RFIM behavior of $\text{Fe}_{1-x}\text{Co}_x\text{Cl}_2$ was investigated experimentally by Wong.² He finds a crossover into RFIM behavior with a crossover exponent $\phi = 1.24 \pm 0.09$. Theoretically Aharony¹⁰ predicted relationships with the order-parameter-susceptibility exponent γ , either $\phi = \gamma$, if the zero-field behavior is dominated by the nonrandom critical behavior, or $\phi > \gamma$, if the critical exponents correspond to the REIM fixed point. Consequently, Wong's value of ϕ seems to correspond to $\gamma_{\text{pure}} = 1.25$,¹¹ rather than to $\gamma_{\text{random}} = 1.34$.¹² However, in our recent linear birefringence, refractive index, and specific-heat studies¹³ we were able to positively

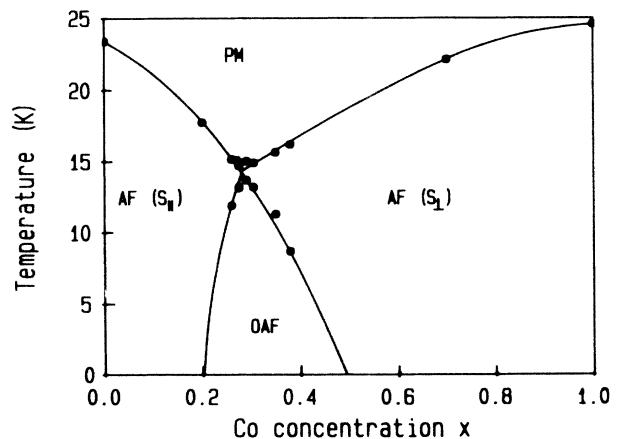


FIG. 1. x vs T phase diagram of $\text{Fe}_{1-x}\text{Co}_x\text{Cl}_2$ as obtained in Ref. 13.

ascertain zero-field random-exchange behavior at least for one concentration, $x = 0.27$. Hence, it seemed to be worthwhile to reexamine the T_c versus H phase line in order to check the value of ϕ , which should then exceed 1.34 after all. As will be reported in this paper, application of the Faraday rotation (FR) method¹⁴ to mixtures with $x = 0.20$ and 0.27 , indeed, yields $\phi = 1.40 \pm 0.05$ and 1.44 ± 0.08 , respectively, thus confirming the theoretical prediction.¹⁰ The obvious discrepancy with Wong's value² may be traced back to both a higher precision in determining T_c versus H and a crucial reduction of the concentration gradients of the samples probed in our optical measurements.

In addition to the critical behavior, GA (Ref. 7) considered multicritical behavior of a ferromagnet with finite anisotropy in a moderate random longitudinal field. They believe that, again, as in the weak-field limit, the random-exchange antiferromagnet like $\text{Fe}_{1-x}\text{Co}_x\text{Cl}_2$ in a uniform field would present a possible experimental realization of this model. However, they pointed out that the critical behavior may not necessarily be the same for both systems. The first experimental investigation of the x - T - H phase diagram of $\text{Fe}_{1-x}\text{Co}_x\text{Cl}_2$ including multicritical points was done by Wood and Day⁵ by means of light scattering. This is due to the walls between AF and PM domains in the mixed phase, which accompanies the spin-flip PT as is well-known from pure FeCl_2 .¹⁵ Qualitatively similar behavior was found⁵ for mixtures with $0 \leq x \leq 0.29$. Accordingly, Wood and Day⁵ inferred metamagnetic behavior for all of these concentrations. On the other hand, neutron scattering data of Wong and Cable⁴ revealed a spin-flop (SF) transition for $x = 0.275$, which seems to be of second order. Light scattering as observed on similar concentrations⁵ must then be due to a spatially inhomogeneous SF phase. Wong and Cable⁴ proposed this to be due to RF originating in the SF phase from the external field. RF-induced domain states, however, are usually known⁹ to be very fine-grained with domain sizes well below the wavelength of visible light. Light scattering should, hence, be very inefficient in a SF domain state.

In order to clarify this unsatisfactory situation we rechecked the H versus T phase diagrams using FR and "transparent" magnetic circular dichroism¹⁵ (TMCD) data. Two concentrations being far and near from the tetracritical value $x_t \sim 0.28$ (based on the scale of our atomic absorption spectroscopy data¹³) were chosen. For $x = 0.20$ we find evidence for spin flip into a mixed phase from both FR and TMCD, whereas $x = 0.27$ gives rise to a phase lacking any TMCD. The occurrence of both situations agrees with the idea⁷ that the admixture of Co^{2+} ions weakens the average Ising anisotropy of FeCl_2 , and thus changes its behavior in a longitudinal field. A full account of the H versus T phase diagrams will be given for both concentrations and discussed with reference to the preceding reports.^{2,4,5} The near-tetracritical case $x = 0.27$ is particularly interesting, since very weak effective Ising anisotropy gives rise to a large extension of the spin-flop region. A pronounced umbilicus appears at the bicritical point,¹⁶ which lies very near to the Néel point, ($T_N, H = 0$).

Another point of interest is the observation of field-induced metastability. In 3D RFIM systems the zero-field cooled (ZFC) state is believed to have long-range order, whereas field cooling (FC) produces metastable domain states.^{9,17} This was, indeed, confirmed experimentally for $\text{Fe}_{1-x}\text{Co}_x\text{Cl}_2$ by Wong and Cable by means of neutron scattering investigations.³ Owing to the domain state the sublattice magnetization appears reduced in FC samples in comparison with that of ZFC samples. Complementarily, our FR measurements reveal enhanced *uniform* magnetization, $M(\text{FC})$, in FC samples compared with that of ZFC ones, $M(\text{ZFC})$. Similar effects were reported previously for the diluted system $\text{Fe}_{0.7}\text{Mg}_{0.3}\text{Cl}_2$,¹⁸ in agreement with model calculations of Soukoulis *et al.*¹⁹ The threshold fields for the onset of positive $\Delta M = M(\text{FC}) - M(\text{ZFC})$, if any, are found to be considerably smaller than those reported for the sublattice magnetization previously.³ In contrast with the neutron results,³ we do not find any time dependence of the metastable FC state.

Evidence of random-field induced metastability was also looked for at the first-order phase boundaries appearing at moderate fields as mentioned above. Indeed, ΔM effects in the sense explained for the second-order RFIM phase line, occur upon crossing both the spin-flop-to-AF ($x = 0.20$) and the SF-to-AF phase boundaries ($x = 0.27$) in isothermal field cycles. These observations agree qualitatively with previous pulsed field experiments on $\text{Fe}_{1-x}\text{Zn}_x\text{F}_2$.²⁰ On the other hand, any ΔM effect is lacking upon crossing the PM-SF phase boundary ($x = 0.27$). The SF domain state observed previously⁴ is, hence, most likely not due to random fields as proposed.⁴ Magneto-crystalline anisotropy, in conjunction with random natural strains, will be discussed to be the origin of this microdomain structure similarly as in the case of the zero-field OAF microdomains.¹³

II. EXPERIMENTAL PROCEDURE

The FR has been measured with a modulation method described by Modine and Major.²¹ Using lock-in technique one detects the second harmonic of the light intensity signal,

$$I_{2\omega} = I_0 J_2(\delta) \cos[2(\theta - \phi)] , \quad (1)$$

with θ and ϕ being the FR rotation and angle between the directions of the analyzer and of the polarizer, respectively. The modulator is operated at a frequency $\omega/2\pi = 50$ kHz and with a phase amplitude $\delta \sim 170^\circ$ for maximum signal-to-noise ratio. J_2 and I_0 denote Bessel's function and the initial intensity of low-power He-Ne laser light ($\lambda = 633$ nm), respectively. We use a compensation method such that $I_{2\omega} = 0$ by adjusting the analyzer to $\phi = \theta - \pi/4$. Angular resolution of better than 1 mdeg is achieved by use of a rotating table (PI, type P038) driven by a stepper motor. The temperature is stabilized to within 3 mK in a special-purpose helium gas-flow cryostat equipped with a superconducting solenoid ($H \leq 45$ kOe). After changing the temperature in steps of no smaller than 4 mK, waiting times of about 25 s before measuring ϕ were allowed for temperature stabilization and sample equilibration.

Detailed information concerning the sample preparation was given previously.¹³ The thickness of the samples is typically 0.2–0.3 mm. We have used diaphragms with a diameter of 0.7 mm, in order to reduce the smearing of the phase transition temperature due to the concentration gradient of typically $\Delta x = 0.012/\text{cm}$ to below $\Delta T_c \sim 1$ mK. For measuring the TMCD we used a standard high-frequency modulation technique.¹⁵ Owing to the doping with CoCl_2 , the samples of $\text{Fe}_{1-x}\text{Co}_x\text{Cl}_2$ are not completely transparent at the wavelength used.²² Hence, finite MCD signals appear in the homogeneous, domain-free phases, without, however, masking the sharp onset of TMCD, which is due to domain walls in the mixed phase.

III. EXPERIMENTAL RESULTS

A. Preliminary remarks

As has been pointed out by Pommier *et al.*,²³ the FR of a transparent antiferromagnet generally depends on both the magnetization M and the local magnetic field H_{loc} according to

$$\theta = aM + bH_{\text{loc}}, \quad (2)$$

where a and b are constants. In antiferromagnets with nonquenched orbital momentum of the ground state the second term in Eq. (2) is usually some orders of magnitude smaller than the first one. This holds for FeCl_2 and CoCl_2 , which via spin-orbit coupling, exhibit strong anisotropy along and perpendicularly to the c axis, respectively. Especially for FeCl_2 , Griffin *et al.*¹⁵ and Dillon *et al.*²⁴ have evidenced the validity of the strict proportionality of θ with M . It seems, hence, justified to presume that this also holds in cases, where $x > 0$. This seems to be proven at least for those mixtures, which order axially, i.e., for $x < x_t \cong 0.28$. As can be seen in Fig. 2 the FR of a sample with $x = 0.20$ clearly exhibits the features of the magnetization of a uniaxial antiferromagnet in a parallel field. Curie-Weiss behavior dominates at high temperatures and θ vanishes as $T \rightarrow 0$. Close resemblance with the parallel susceptibility as measured by Wong *et al.*¹ on samples with $x = 0.1625$ and $x = 0.2641$ is obvious. This holds, too, for the case $x = 0.70$ (Fig. 2), which is comparable with the χ_1 versus T results of Wong *et al.* of samples with $x = 0.6035$ and 0.8011 , respectively.

Recent scaling considerations¹⁴ of the 3D Ising antiferromagnet in a uniform field reveal, for the temperature derivative of the magnetization,

$$(\partial M / \partial T)_H \propto H^y |t|^{-\tilde{\alpha}}, \quad (3)$$

with the RFIM critical exponents y and $\tilde{\alpha}$, the reduced temperature $t = [T - T_c(H)]/T_N$ and the Néel temperature T_N . Hence, the maximum of $d\theta/dT$ unambiguously defines the PT temperature as shown in Fig. 2 for $x = 0.20$ and $H = 2.56$ kOe. θ versus T curves thus conveniently enable us to study the critical behavior near T_c . In order to investigate the H - T phase boundaries in the spin-flip ($x = 0.20$) or SF ($x = 0.270$) region, it proves convenient to study θ versus H curves at constant tem-

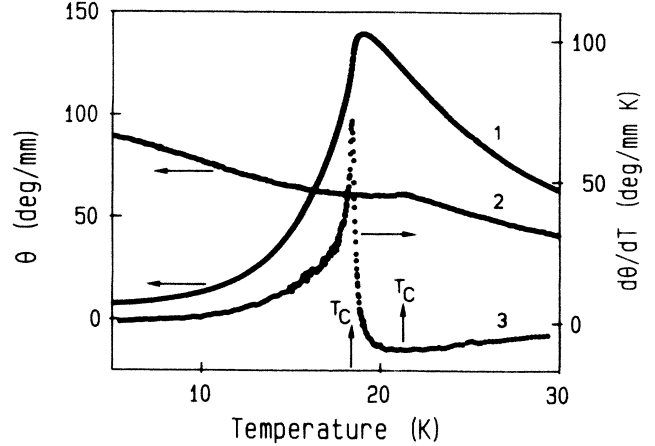


FIG. 2. θ vs T of $\text{Fe}_{0.8}\text{Co}_{0.2}\text{Cl}_2$ (curve 1) and $\text{Fe}_{0.3}\text{Co}_{0.7}\text{Cl}_2$ (curve 2) measured with $\lambda = 633$ nm in axial fields $H = 2.56$ and 5.18 kOe, respectively. Curve 3 shows the derivative, $d\theta/dT$ vs T of curve 1. The respective phase transition temperatures, T_c , are indicated by arrows.

perature. In general, sharp features of $(\partial\theta/\partial H)_T$ will define the phase boundaries as was discussed in the case of spin-flipping FeCl_2 .²⁴ Similar singularities are also expected in the SF case. It should be noted that θ versus H curves are not suitable for studying *critical* behavior in the RFIM regime. Since the critical temperature varies as

$$T_c(H) = T_N - AH^2 - BH^{2/\phi}, \quad (4)$$

where A and B denote the mean-field and the random-field contributions with ϕ being the crossover exponent,^{6,9} it is obvious from relation (3) that critical exponents are not unambiguously obtained from isothermal field scans unless A and B are very precisely known.

The TMCD method¹⁵ used to determine the external field boundaries of the spin-flip PT is believed to be equivalent to the light-scattering method used by Wood and Day.⁵ In both experiments elastic light scattering at the domain walls between the AF and the PM phases is involved. Measurable effects require domain sizes of the order of the light wavelength.

B. FR and TMCD

From the phase diagram in zero applied field it is well known¹ that $\text{Fe}_{1-x}\text{Co}_x\text{Cl}_2$ behaves like a 3D Ising antiferromagnet for $x < x_t$ and like a 3D xy antiferromagnet for $x > x_t$ at the upper PT's. These are described by S_{\parallel} and S_{\perp} ordering, respectively. It is, hence, meaningful to discuss our results separately for both cases. In particular, the appearance of linear birefringence¹³ (LB) has to be taken into account in order to explain some of the experimental results in the case $x > x_t$.

1. $x < x_t$

Figures 3 and 4 show θ versus T data for $x = 0.20$ and 0.27 , respectively, in the vicinity of $T_c(H)$ for various rel-

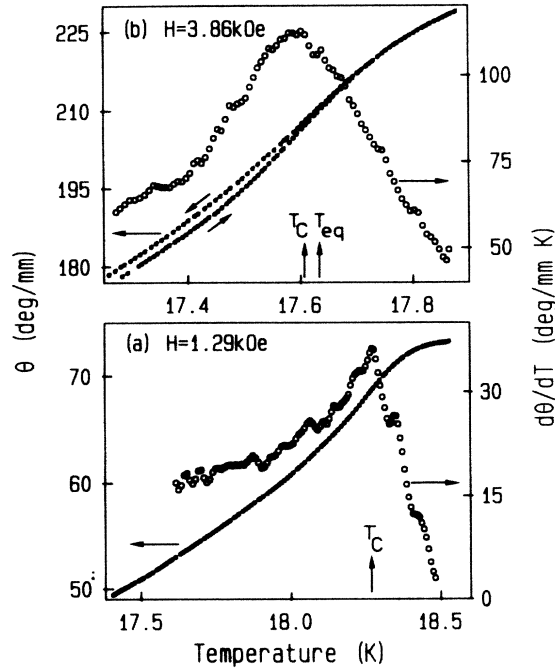


FIG. 3. θ and $d\theta/dT$ vs T of $\text{Fe}_{0.8}\text{Co}_{0.2}\text{Cl}_2$ for (a) $H = 1.29$ kOe and (b) 3.86 kOe, where the temperature was cycled around $T_c = 17.60$ K and $T_{eq} = 17.64$ K (arrows) after ZFC.

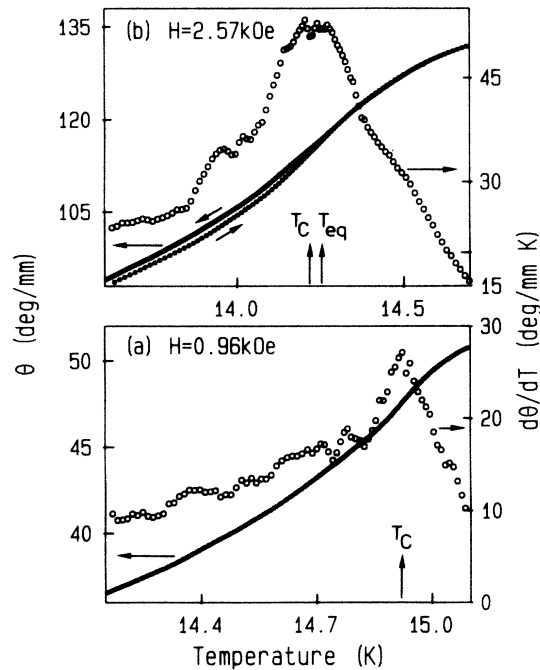


FIG. 4. θ and $d\theta/dT$ vs T of $\text{Fe}_{0.73}\text{Co}_{0.27}\text{Cl}_2$ for (a) $H = 0.96$ kOe and (b) 2.57 kOe, where the temperature was cycled around $T_c = 14.21$ K and $T_{eq} = 14.25$ K (arrows) after ZFC.

atively weak magnetic fields, $1 \text{ kOe} \lesssim H \lesssim 4 \text{ kOe}$. It is observed that FC yields larger FR, hence, enhanced magnetization, $\Delta M > 0$, than field heating after ZFC above certain threshold field values ($H \gtrsim 2.25$ kOe and $\gtrsim 1$ kOe for $x = 0.20$ and 0.27 , respectively). This is depicted in Fig. 3(b) for $x = 0.20$ and $H = 3.86$ kOe and in Fig. 4(b) for $x = 0.27$ and $H = 2.57$ kOe. As will be discussed in Sec. IV B, the occurrence of $\Delta\theta \propto \Delta M$ is connected with the fact that a domain state develops in FC samples, whereas ZFC samples exhibit antiferromagnetic long-range order.^{9,17,19,25} This was investigated by Wong and Cable³ on $\text{Fe}_{1-x}\text{Co}_x\text{Cl}_2$ with $x = 0.255$ and 0.285 by means of neutron scattering.

Another important fact is the increase of rounding of the $d\theta/dT$ curves in Figs. 3 and 4 on increasing the field. We refer to this point in the discussion. As pointed out above we obtain the H versus T phase line from the peaks of $d\theta/dT$ versus T . For weak fields these lines, plotted as H^2 versus T for $x = 0.20$ and 0.27 , are depicted in Fig. 5. Anticipating results obtained from θ versus H curves to be discussed below, in the case $x = 0.27$ only field values below the bicritical one, $H_b \simeq 1.5$ kOe, have to be taken into account. The concave curvatures arise from the crossover from REIM to RFIM behavior according to Eq. (4). Following Wong,² $A(x)$ is determined as

$$A(x) = A(0)T_N(0)/T_N(x), \quad (5)$$

involving the Néel temperature $T_N(0) = 23.55$ K of pure FeCl_2 . Since our sample dimensions are nearly identical to those used by Wong,² we adopt $A(0) = 0.0149$ (kOe),² and obtain, by using least-squares fits, $\phi = 1.40 \pm 0.05$ for $x = 0.20$ and $\phi = 1.44 \pm 0.08$ for $x = 0.27$, respectively.

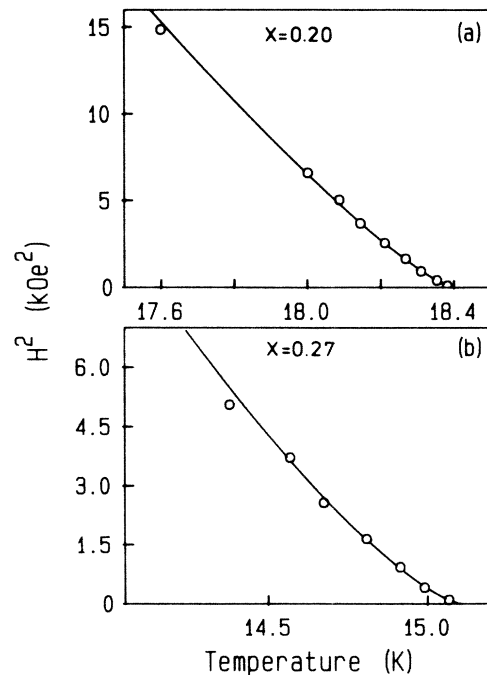


FIG. 5. H^2 vs $T_c(H)$ phase diagram of ZFC (a) $\text{Fe}_{0.8}\text{Co}_{0.2}\text{Cl}_2$ and (b) $\text{Fe}_{0.73}\text{Co}_{0.27}\text{Cl}_2$, best fitted to Eq. (4) (solid lines) for $H^2 \leq 15$ and 3 kOe², respectively (see text).

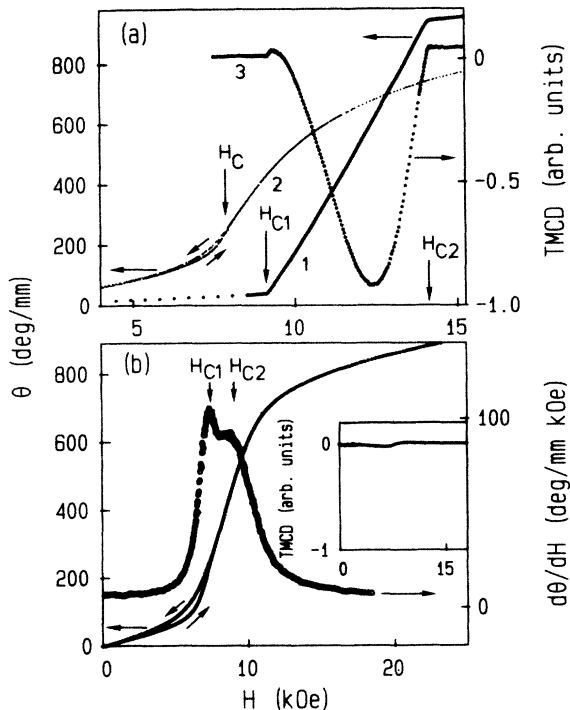


FIG. 6. (a) θ vs H of $\text{Fe}_{0.8}\text{Co}_{0.2}\text{Cl}_2$ for $T=7.00$ K (curve 1) and 14.44 K (curve 2). The TMCD vs H is depicted for $T=7.00$ K by curve 3. (b) θ , $d\theta/dH$ (ZFC), and TMCD (inset) vs H of $\text{Fe}_{0.73}\text{Co}_{0.27}\text{Cl}_2$ for $T=4.36$ K. The lower and upper fields, H_{c1} and H_{c2} , of the spin-flip and spin-flop transitions are indicated by arrows in (a) and (b), respectively. Field cycles around $H_c=7.97$ kOe (arrow) for $\text{Fe}_{0.8}\text{Co}_{0.2}\text{Cl}_2$ at (a) 14.44 K and around $H_{c1}=7.29$ kOe for $\text{Fe}_{0.73}\text{Co}_{0.27}\text{Cl}_2$ at (b) 4.36 K are denoted by arrows.

We have fitted our data within $17.5 \text{ K} < T < 18.398 \text{ K} = T_N(0.20)$ and $14.7 \text{ K} < T < 15.109 \text{ K} = T_N(0.27)$ for $x=0.20$ and 0.27 , respectively. In the case $x=0.20$, tentatively also, demagnetization was taken into account which was obtained experimentally from low- T θ versus H data (see below). Clearly this procedure yields a larger value $A(0) \sim 0.023$ (kOe).² However, the least-squares fit for the phase boundary thus obtained, H_i versus T , again gives $\phi = 1.40 \pm 0.05$.

In order to investigate the multicritical behavior⁷ we have measured θ and TMCD versus H for both the fairly low and the nearly tetracritical concentrations, $x=0.20$ and 0.27 , respectively. Fig. 6(a) refers to $x=0.20$ and shows θ versus H for $T=7.00$ K (curve 1), $T=14.44$ K (curve 2), and the TMCD versus H for $T=7.00$ K (curve 3). The magnetization curve for $T=7.00$ K is typical for a metamagnet.²⁶ Within the AF phase ($H < H_{c1}$), the magnetization is small and varies linearly with H . A steep change of the slope occurs within the spin-flip region ($H_{c1} \leq H \leq H_{c2}$), where AF and PM domains coexist, until for $H > H_{c2}$ the magnetization saturates rapidly. $H_{c1}=9.17$ kOe and $H_{c2}=14.13$ kOe denote the lower and the upper critical field, respectively, of the mixed phase and are indicated by arrows in Fig. 6(a). Within

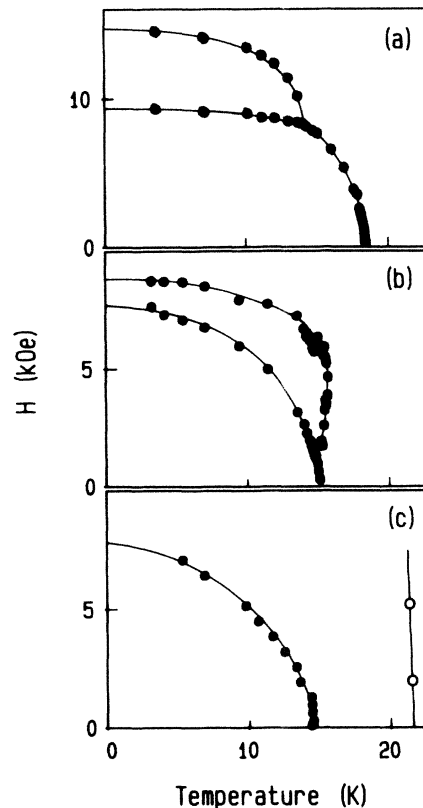


FIG. 7. H vs T phase diagrams of $\text{Fe}_{1-x}\text{Co}_x\text{Cl}_2$ as deduced from FR data for (a) $x=0.20$, (b) 0.27 , and (c) 0.315 (solid circles) and 0.70 (open circles), interpolated by eye-guiding solid lines.

the spin-flip region the internal magnetic field is constant. This enables us to determine the demagnetization factor N according to

$$H_i = H_{c1} - \theta_{c1}N = H_{c2} - \theta_{c2}N, \quad (6)$$

where θ_{c1} and θ_{c2} denote the FR at H_{c1} and H_{c2} , respectively. We obtain $N=0.017$ kOe/deg as used for determining ϕ (see above).

The spin-flip transition gives rise to TMCD as shown in Fig. 6(a). The shape of the TMCD curves is due to uncontrolled domain formation. Therefore occasionally smooth onsets may be encountered [Fig. 6(a), $H \sim H_{c1}$]. However, by use of both θ and TMCD versus H , eventually taken at different sample sections, the phase boundaries emerge with sufficient accuracy. H_{c1} and H_{c2} data taken this way at temperatures $3.5 \text{ K} < T < 14.4 \text{ K}$ are plotted in Fig. 7(a). They constitute the lower part of the phase diagram, splitting into two lines below the tricritical point ($T_t \approx 13.93 \text{ K}$, $H_t \approx 8.3 \text{ kOe}$). Above that point the θ versus H curves vary smoothly and indicate second-order PT's by virtue of inflexion points as shown for $T=14.44$ K in Fig. 6(a) (curve 2), where $H_c=7.97$ kOe. These points belong to the AF-PM phase boundary, which can also be constructed from θ versus T data as described above. Data points obtained within $T_l < T < T_N$ from both of these techniques are plotted in Fig. 7(a).

Upon cycling the field through H_c , enhanced FR, $\Delta\theta$ is observed just below the phase transition at $H_c = 7.97$ kOe. The effect is relatively small and vanishes at higher temperatures. It is attributed to domain states due to RF,⁹ which emerge at $H \leq H_c$. Evidently, metastabilities arise whenever the RFIM phase boundary H versus T is crossed,²⁰ either taking isothermal [Fig. 6(a)] or isomagnetic scans (Figs. 3 and 4, respectively).

For $x = 0.27$, we systematically measured θ versus H in the temperature range $3.5 \text{ K} < T < 16.2 \text{ K}$. Several of these curves and their derivatives, $d\theta/dH$ versus H , referring to $T = 4.36, 13.52, 14.98, 15.51,$ and 16.20 K , are plotted in Figs. 6(b) and 8(a)–8(d), respectively. It is seen that steep changes of θ versus H , corresponding to sharp peaks of $d\theta/dH$ versus H , occur at fairly low fields, $3 \text{ kOe} \lesssim H_{c1} \lesssim 8 \text{ kOe}$, at temperatures $14 \text{ K} \geq T \geq 4 \text{ K}$ [Figs. 6(b) and 8(a)]. They obviously hint at the occurrence of PT's. Contrary to the behavior of the $x = 0.20$ sample, however, we do not find TMCD at any temperature or field value [see inset of Fig. 6(b) for an example; small bumps are due to ordinary MCD owing to residual absorption at $\lambda = 633 \text{ nm}$]. Hence, macroscopical homogeneity of the phase at $H \geq H_{c1}$ is inferred and, in particular, a mixed phase as found for $x = 0.20$ is safely excluded to occur at $x = 0.27$. In accordance with theoretical conjectures,⁷ we, hence, conclude that H_{c1} marks a SF PT, where χ_{\parallel} should diverge.²⁶ Owing to demagnetization, however, in real measurements reduced values $\chi_{\parallel}(H_{c1}) = 1/N$ are expected.²⁶ Since $\chi_{\parallel} = C(d\theta/dH)$, with C being a nearly temperature independent factor,²⁴ constant peak values of $d\theta/dH$ are expected along the AF-SF phase boundary. However, these are observed to decrease significantly from 120 to 55 deg/mm kOe for $3.5 \text{ K} < T < 14.8 \text{ K}$ [cf. Figs. 6(b) and 8(a)]. This might indicate smearing of the expected⁷ first-order SF transitions, becoming more important with increasing temperature as will be discussed in terms of RF effects²⁷ in Sec. IV B. It should be mentioned, however, that the SF transition might well be interpreted as being second order, too. This possibility was concluded by Wong and Cable⁴ from their neutron data of an $x = 0.275$ sample. On the other hand, in our opinion, the observed⁴ very steep variation of M_{\parallel} versus H at H_{c1} also very much resembles a first-order discontinuity, albeit slightly smeared. Much clearer evidence in favor of a first-order AF-SF transition was recently found for the related undiluted RF system $\text{Fe}_{1-x}\text{Ni}_x\text{Cl}_2$ at the near-tetracritical concentration $x = 0.85$.²⁸

The upper critical field, H_{c2} , appears worse defined than H_{c1} , owing to the lack of sharp kinks in θ versus H as seen in Figs. 6(b) and 8(a). However, since the SF phase is expected to yield a horizontal and flat χ_{\parallel} versus H curve up to H_{c2} ,²⁶ this field may tentatively be defined as the endpoint of the flat horizontal portion of the derivative curves $d\theta/dH$ versus H . This is indicated in Figs. 6(b) and 8(a) by horizontal lines and arrows at $H_{c2} = 8.70$ and 7.02 kOe , respectively. Possible reasons for the rounding, which was recently also observed on the magnetization of $\text{Fe}_{1-x}\text{Ni}_x\text{Cl}_2$,²⁸ will be discussed below.

On approaching $T \sim 14.8 \text{ K}$ from below, the peak of $d\theta/dH$ at H_{c1} rapidly flattens out, and the initial slope is

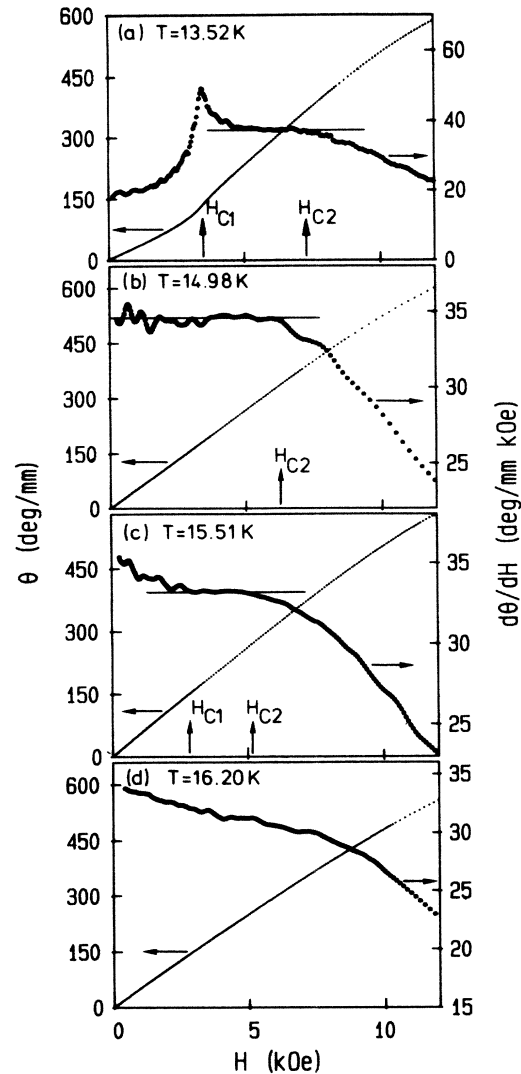


FIG. 8. θ and $d\theta/dH$ vs H of $\text{Fe}_{0.73}\text{Co}_{0.27}\text{Cl}_2$ for (a) $T = 13.52 \text{ K}$, (b) 14.98 K , (c) 15.51 K , and (d) 16.20 K . Spin-flop phases between H_{c1} and H_{c2} (arrows) are characterized by $d\theta/dT = \text{const}$ as indicated by horizontal solid lines.

gradually lifted up to the flat part of the SF phase. This is why within $14.8 \text{ K} < T < 15.2 \text{ K}$ only the H_{c2} point is clearly conceivable [Fig. 8(b)]. Large scatter of the data precludes any clearcut information on the low-field range. It is in that temperature range, where the second-order RFIM PT is clearly found from θ versus T scans at fields $H \lesssim 1.5 \text{ kOe}$ [Fig. 5(b)]. Unfortunately, the PM-SF phase boundary is unrevealed by θ versus T scans, which merely show broad peaks at the location of $T(H_{c2})$ [see, e.g., Fig. 4(b)].

A common plot of the RFIM phase line together with all H_{c1} and H_{c2} values obtained thus far in Fig. 7(b) shows the presence of the bicritical point (BCP) at $T_b = 14.6 \pm 0.02 \text{ K}$ and $H_b = 1.50 \pm 0.1 \text{ kOe}$. Unfortunately, as explained above, essential H_{c1} data are lacking, which would be needed to determine the BCP more precisely. However, the typical balloon-like part of the SF region^{16,29} is clearly found at higher temperatures,

15.2 K < T < 15.75 K, where both H_{c1} and H_{c2} emerge again from the horizontal plateau of $d\theta/dH$ versus H [Fig. 8(c)]. Here, the SF phase separates high and low susceptibility PM phases being stable at $H < H_{c1}$ and $H > H_{c2}$, respectively. Owing to the roundings at both ends of the $d\theta/dH$ plateau, the critical field values H_{c1} and H_{c2} can be determined only within large error margins $\delta H \sim \pm 0.5$ kOe. This explains the larger scatter of the data points in Fig. 7(b). Very clearly, however, the plateau shrinks rapidly as T is raised and vanishes for $T > 15.7$ K. This is shown for $T = 16.2$ K in Fig. 8(d). A full account of the phase diagram thus obtained will be given in Sec. IV B.

2. $x > x_t$

Typical θ versus T data for S_{\perp} ordering $\text{Fe}_{1-x}\text{Co}_x\text{Cl}_2$ with a nearly tetracritical concentration are shown in Fig. 9 for $x = 0.315$ at $H = 0.19$ and 5.14 kOe. As was shown in our previous papers,¹³ appreciable intraplanar LB is found at $x > x_t$ due to the spontaneous in-plane spin-ordering occurring below T_{c1} . It is well-known, that the measured circular birefringence is a superposition of both FR and LB. Drastic effects in cases, where the phase shifts due to LB and FR are of the same order of magnitude, were reported by Tabor and Chen.³⁰ This must be taken into account when discussing the measured FR versus T curves in Fig. 9. For example, hysteresis is found below $T \sim 13.3$ K for $H = 0.19$ kOe [arrow denoted as T_{c2} in Fig. 9(a)]. This temperature coincides exactly with that found in the zero-field LB versus T curve, and corresponds to the transition temperature T_{c2} into the OAF phase.¹³ On the other hand, T_c as determined from the maximum slope of the FR versus T curve [arrow denoted as T_c, T_{c1} in Fig. 9(a)] seems to agree with T_{c1} as obtained from the LB in the limit $H \rightarrow 0$.¹³ Only these T_{c1} values are used to construct the H versus T phase diagram [Fig. 7(c)]. It consists of a strongly bent single curve, ending at $H_c \sim 7.5$ kOe in the limit $T \rightarrow 0$. No further high-field PT is expected, since H lies nonparallel to the easy spin direction.

In the low-field limit $H \lesssim 0.8$ kOe, our T_c values prove to be virtually constant. This is believed to be an artifact due to the superposition of FR and LB, thus ruling out any serious analysis of the expected² low-field crossover behavior. On increasing the field, on the other hand, the FR increases rapidly. For $H > 5$ kOe [Fig. 9(b)] the θ versus T curves resemble those obtained at $x < x_t$ (Figs. 3 and 4). This shows that the influence of the LB is largely suppressed. It is interesting to note that, again, enhanced magnetization occurs upon FC. This might indicate random fields, creating domain state OAF phases upon FC.

As an example for the random intraplanar exchange regime, we present the θ versus T curve for $x = 0.70$ and $H = 5.18$ kOe in Fig. 2 in comparison with that for $x = 0.20$ and $H = 2.56$ kOe. Obviously, owing to the different zero-field spin symmetries (Fig. 1) these curves are related to χ_{\perp} versus T for $x = 0.70$ and to χ_{\parallel} versus T for $x = 0.20$, respectively, as measured by Wong *et al.*¹ at similar concentrations. At $x = 0.70$ only a small anomaly arises near T_c , which may be used to construct

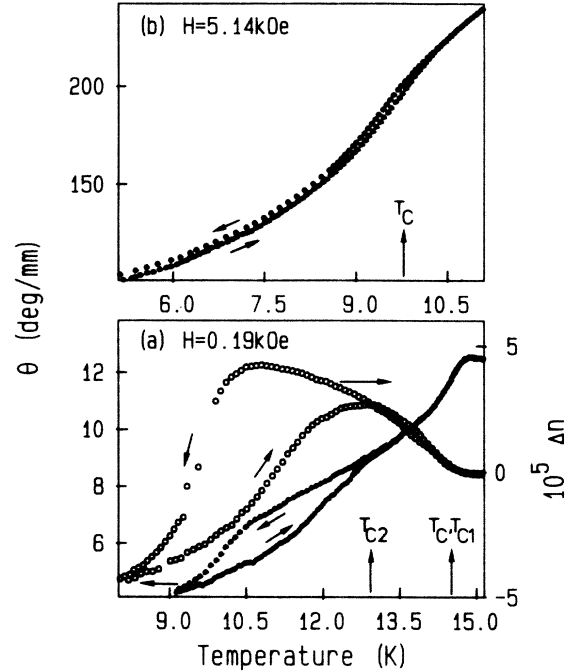


FIG. 9. θ vs T (solid circles) of $\text{Fe}_{0.685}\text{Co}_{0.315}\text{Cl}_2$ cycled around (a) $T_c = 14.52$ K for $H = 0.19$ kOe and around (b) $T_c = 9.80$ K for $H = 5.14$ kOe are compared with the zero-field c -plane birefringence [(a), open circles], which evidences transitions at $T_{c1} \sim T_c$ (0.19 kOe) and at $T_{c2} = 12.95$ K (see Ref. 13). Field cycles and transition temperatures are indicated by arrows.

the H versus T phase diagram [Fig. 7(c)]. Comparatively small shifts ($\Delta T_c = -1.3$ K for $H = 35$ kOe) are found. They are compatible with c_m data of Wong² ($\Delta T_c = -1.2$ K for $x = 0.604$ and $H = 19$ kOe). The differences of the specific shift values $\Delta T_c / \Delta H$, obtained in both experiments are due to the different concentrations involved.

IV. DISCUSSION

A. Random-field behavior

In the following we shall discuss our experimental results on $\text{Fe}_{1-x}\text{Co}_x\text{Cl}_2$ with respect to its RFIM behavior. FA (Ref. 6) have shown that one possible realization of a RFIM system is given by a uniaxial anisotropic antiferromagnet with random exchange constants in a uniform magnetic field. They mention explicitly that $\text{Fe}_{1-x}\text{Co}_x\text{Cl}_2$ in the S_{\parallel} -ordered concentration range might be a good candidate for this situation.

Their consideration is based on a two-sublattice Hamiltonian of the form

$$H = -\frac{1}{2} \sum_{k,l} [J_{kl}^{\parallel} S_k^{\parallel} S_l^{\parallel} + J_{kl}^{\perp} (\mathbf{S}_k \cdot \mathbf{S}_l - S_k^{\parallel} S_l^{\parallel})] - \sum_l \mu H S_l^{\parallel}, \quad (7)$$

involving antiferromagnetic random exchange coupling coefficients J_{kl}^{\parallel} and J_{kl}^{\perp} parallel and perpendicularly, respectively, to the c axis and acting on the respective components of the spins \mathbf{S}_k and \mathbf{S}_l . The external field H acts only on the parallel spin components S_l^{\parallel} . Mukamel³¹ pointed out that the present system exhibits off-diagonal coupling terms for symmetry reasons. These were neglected by FA.⁶ In our previous paper¹³ we have shown that finite off-diagonal correlations, indeed, appear in zero-field, albeit in a smeared fashion and slowly growing below T_{c1} , and thus noncontributing to the critical behavior at T_{c1} . One might, hence, argue that also for finite small fields all off-diagonal terms will remain non-critical and can henceforth be neglected within the approach of FA.⁶

According to Eq. (4) the random fields give rise to crossover from REIM to RFIM behavior. The corresponding exponent ϕ is predicted¹⁰ to satisfy the relation $\phi/\gamma_{\text{random}} \simeq 1.05-1.1$. With $\gamma_{\text{random}} = 1.34$ (Ref. 12) and our experimental results $\phi = 1.40$ and 1.44 for $x = 0.20$ and 0.27 , respectively, we obtain $\phi/\gamma_{\text{random}} \simeq 1.05-1.08$ in satisfactory agreement with the above-mentioned theoretical result. On the other hand, Wong² found $\phi = 1.24 \pm 0.09$ for $\text{Fe}_{0.714}\text{Co}_{0.286}\text{Cl}_2$. In order to explain this relatively small value, he assumed "weak randomness," which would yield $\phi = \gamma_{\text{pure}}$, where $\phi_{\text{pure}} = 1.25$.¹¹ However, as shown in our previous paper,¹³ mixtures like $\text{Fe}_{0.73}\text{Co}_{0.27}\text{Cl}_2$ very clearly exhibit REIM behavior as verified by negative specific-heat exponents, $\alpha \simeq -0.11$. Hence, "weak randomness" must be discarded. As pointed out recently in a similar discussion on the RFIM behavior of $\text{Fe}_{0.7}\text{Mg}_{0.3}\text{Cl}_2$,¹⁸ we rather believe that erroneous H versus T phase lines systematically were deduced from the C_m versus T data² taken on macroscopic samples containing concentration gradients. This was predicted by Belanger *et al.*,³² who recently³³ also presented convincing model investigations towards these ends. Since our data were taken on very small sample volumes ($\sim 10^{-3}$ mm³) using a narrow laser beam of 0.7 mm diameter, our analysis can be assumed to be essentially free from these errors.

In the RFIM regime the temperature derivative of the FR is expected to diverge according to Eq. (3) as $(\delta\theta/\delta T)_H \propto |t|^{-\alpha}$. Previous investigations on $\text{Fe}_{1-x}\text{Zn}_x\text{F}_2$ (Ref. 14) and $\text{Fe}_{1-x}\text{Mg}_x\text{Cl}_2$ (Ref. 18) suggested $\alpha \sim 0$, i.e., logarithmic divergences. Semilogarithmic plots, $(d\theta/dT)$ versus $\log_{10}|t|$, with $t = [T - T_c(H)]/T_N$, should, hence reveal *one* single straight line. This condition, however, is fulfilled only in fairly large fields. As shown in Fig. 10(c), this applies approximately to the range $-2.5 \leq \log_{10}|t| \leq -2.0$ for $H = 7.71$ kOe and $x = 0.20$. At this nearly tricritical field ($H_t \simeq 9.1$ kOe) rounding occurs very near to T_c ($\log_{10}|t| < -2.5$). This may tentatively be traced back to dynamical effects^{9,14,18} (uncomplete equilibration within the time scale of our FR measurements, $\tau \sim 25$ s). On reducing the field the linear parts of $d\theta/dH$ versus $\log_{10}|t|$ are shrinking and the curves are gradually bent downward in the whole range of t values [Fig. 10(b), referring to $H = 3.86$ kOe]. Eventually, they split into two branches, $T < T_c$ data becoming larger than those

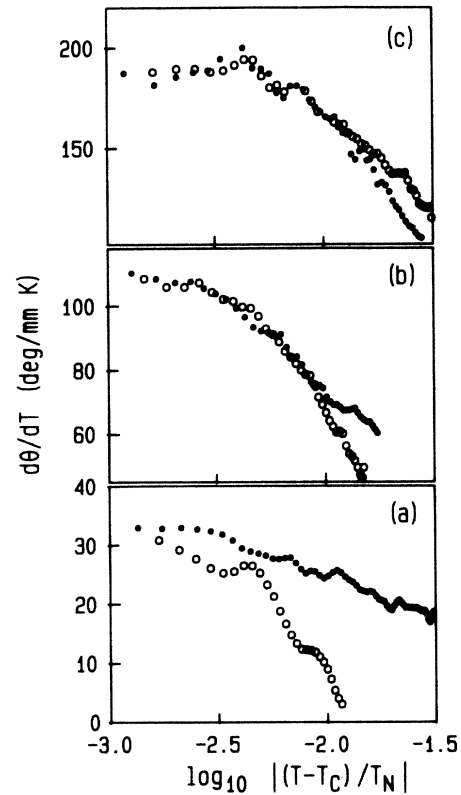


FIG. 10. $d\theta/dT$ vs $\log_{10} |(T - T_c)/T_N|$ of $\text{Fe}_{0.8}\text{Co}_{0.2}\text{Cl}_2$ for (a) $H = 1.29$ kOe, (b) 3.86 kOe, and (c) 7.71 kOe. Open circles, $T > T_c$; solid circles, $T < T_c$, where (a) $T_c = 18.27$ K, (b) 17.60 K, and (c) 15.18 K.

obtained at $T > T_c$ [Fig. 10(a), referring to $H = 1.29$ kOe]. This behavior is also known from $d\Delta n/dT$ and c_m versus $\log_{10}|t|$ plots at $H = 0$.¹³ It is typical for REIM critical behavior. At intermediate fields [Fig. 10(b)], a typical REIM-to-RFIM crossover situation seems to be encountered. It should be noted that no efforts were made to analyze the $d\theta/dT$ versus T data for $x = 0.27$, since in that case the second-order RFIM phase boundary ends at very low fields, $H \lesssim H_b \simeq 1.5$ kOe (Fig. 7, curve 3).

Finally we come back to the observation of enhanced magnetization as measured upon FC for $H \gtrsim 2.25$ kOe and $H \gtrsim 1$ kOe for $x = 0.20$ and 0.27 , respectively (Figs. 3 and 4). Similar results were obtained on the diluted system $\text{Fe}_{0.7}\text{Mg}_{0.3}\text{Cl}_2$,¹⁸ in accordance with mean-field predictions of Soukoulis *et al.* and Grest *et al.*¹⁹ They found decreasing threshold values of H for the observability of metastable states with increasing randomness in accordance with our observations. The ΔM effect is attributed to the formation of metastable domain states occurring under FC conditions at temperatures $T < T_{\text{eq}}$, where $T_{\text{eq}} \gtrsim T_c$. Experimentally we find a maximum of ΔM at $T_m < T_c$, where $|T_c - T_m| \sim |T_{\text{eq}} - T_c|$.

Clearly, the ΔM (or $\Delta\theta$) effect must be traced back to the presence of domain walls, whereas $M(\text{ZFC})$ is a pure bulk property. In the Ising limit, the wall width is of the order of one lattice spacing, hence, leading to a surface energy per lattice site of the order J . In diluted systems

this energy may be diminished by establishing the walls within regions containing preponderantly nonmagnetic impurities.²⁵ In a competing anisotropy system like $\text{Fe}_{1-x}\text{Co}_x\text{Cl}_2$, a similar effect may arise, if the walls are pinned at regions with high local Co^{2+} concentration. In any case, in order to minimize the Zeeman energy due to the external field, the parallel spin pairs joining at the wall will necessarily align with H . This configuration will establish automatically during domain formation, and thus store excess magnetization, ΔM , in the domain walls. Since $\Delta M \propto NV$, where, $N \propto nR^2$ and $V \propto nR^3$ are the total number of wall sites and the volume of the sample, respectively, subdivided into n domains with average radius R , one easily finds $\Delta M \propto R^{-1}$. Deviations from this simple relation are expected very near to T_c , where the domains are fuzzy^{34,35} and, hence, the relation $N \propto nR^2$ may be violated.

B. Multicritical behavior

The FR measurements for $x = 0.20$ and 0.27 reveal the theoretically predicted⁷ crossover from spin-flip ($x = 0.20$) to spin-flop ($x = 0.27$) behavior on increasing x . Its origin is the decrease of the strong Ising-like anisotropy of FeCl_2 by the admixture of CoCl_2 , which exhibits in-plane anisotropy. The phase diagram for $x = 0.27$ [Fig. 7(b)] is very similar to that of ordinary SF systems, e.g., GdAlO_3 ,²⁹ whose SF phases typically extend to temperatures beyond that of the bicritical point (BCP), $T > T_b$. Somewhat unusually, in our case, the spin-flop phase seems to extend to even $T > T_N$. We think this to be due to the very weak anisotropy, which characterizes the near-tricritical mixtures of $\text{Fe}_{1-x}\text{Co}_x\text{Cl}_2$. According to Shapira,¹⁶ at the BCP the competing easy-axis and the field-induced easy-plane anisotropies cancel each other. The bicritical field H_b is essentially given by²⁶ $H_b^2 \propto k(1-k)$, where $k = D/J$ is the ratio between the constants of the effective uniaxial anisotropy and the isotropic exchange, D and J , respectively. Clearly, $H_b \rightarrow 0$ for $k \rightarrow 0$, which is expected to occur when $x \rightarrow x_t$. Hence, in this limit the BCP, (T_b, H_b) , will shift towards $(T_N, H = 0)$ and the fluctuation-induced umbilicus¹⁶ must appear very pronounced allowing for SF states being stable up to $T \sim 1.05T_N$.

The phase transitions into the SF range merit some further remarks. First of all, there seems to be disagreement concerning their order at the AF-SF phase boundary. Whereas our data ($x = 0.27$) suggest rather sharp first-order jumps [Figs. 6(b) and 8(a)], Wong and Cable⁴ report on continuous (second-order or smeared) transitions ($x = 0.275$). Several mechanisms might explain the observed smearing effects: (i) demagnetization (not accounted for in Ref. 4) creates finite transition intervals on the H scale [cf. Figs. 6(b) and 8(a)], (ii) concentration gradients are present in the relatively large samples used for neutron scattering⁴ and will smear all phase boundaries of the mixed system, (iii) deviation from exact parallelity of \mathbf{H} with respect to the c axis may have misled the system out of the SF shelf.²⁹ Since all of these artifacts were carefully avoided in our experiments, we presume the SF

transitions to be of first order.

The H versus T phase diagrams determined previously by means of neutron scattering⁴ and specific-heat measurements,² respectively, were both reported to exhibit SF phases. The (approximate) BCP coordinates, (12.5 K, 7 kOe) and (14.5 K, 5 kOe) for nominal concentrations $x = 0.275$ and $x = 0.286$, respectively, when compared with those of our $x = 0.27$ sample, (15.4 K, 1.5 kOe), seem to indicate that they refer to intermediate concentrations, $0.20 < x < 0.27$ (on our scale). Indeed, in agreement with the GA theory,⁷ T_b (H_b) is expected to increase (decrease) on reducing the effective uniaxial anisotropy, i.e., for $x \rightarrow x_t$.

Unfortunately none of the phase diagrams of $\text{Fe}_{1-x}\text{Co}_x\text{Cl}_2$ reported up to this date provides evidence for the predicted⁷ gradual onset of a low-temperature SF phase, the critical end point (CEP) of which (T_e, H_e) , lies on the spin-flip phase line, i.e., $T_e < T_t$. On decreasing the anisotropy the CEP merges into the TCP, i.e., $T_e \rightarrow T_t$ ("new multicritical point"⁷) and eventually becomes a BCP. It seems to us that all the multicritical points emerging from our $x = 0.20$ data [Fig. 7(a)] and from those reported by Wood and Day⁵ are TCP's reflecting the strong-anisotropy case ($a \leq 0.5$ in terms of Ref. 7). Neither TMCD nor light scattering⁵ hint at an AF-SF first-order transition at temperatures below T_t , which decreases continuously down to $T_t \sim 7$ K on increasing x up to $x = 0.29$ (on the scale of Ref. 5). Both optical techniques are expected to yield much smaller signals in the nearly homogeneous SF phase (see discussion below) than in the coarse-grained mixed AF-PM phase. On the other hand, neither our $x = 0.27$ data [Fig. 7(b)] nor those obtained by Wong *et al.*^{2,4} give hints at spin-flip behavior above T_b (as would be expected for intermediate anisotropy, $0.5 < a < 0.8$ in terms of Ref. 7). Hence, these experiments seem to reflect the low-anisotropy case ($0.8 < a < 1$ in terms of Ref. 7) with purely bicritical behavior as discussed above. The very existence of a CEP separating low- T SF from high- T spin-flip phases remains, hence, to be shown in experiments on appropriate intermediate concentrations. Presumably these will cover only a very small range within the interval $0.20 < x < 0.27$ on our scale.

A further point of interest is the possible relevance of RF onto the phase boundaries of $\text{Fe}_{0.73}\text{Co}_{0.27}\text{Cl}_2$. At the low-field AF-SF boundary hysteresis of the θ versus H curves occurs upon field cycles [Fig. 6(b)]. Closer inspection reveals that the hysteresis loops seem to start just at the upper bound of the demagnetization-stretched AF-SF transition (see Sec. III B). Hence, this may be considered as a natural feature of the expected⁷ first-order PT. However, on decreasing H , appreciable enhancement of the FR persists far into the AF phase. This reminds us of the $\Delta\theta$ effect found in temperature or field scans across the AF-PM boundary in the RFIM regime [see, e.g., Figs. 3(b), 4(b), and 6(a)]. This was explained in Sec. IV A by RF induced domain states with enhanced domain-wall FR. We believe that a similar mechanism takes place at the SF-AF PT, where random fields due to random exchange and local magnetization act on the staggered magnetization of the AF phase in the same way as at the

PM-AF second-order phase line. Note that the validity of these arguments does not depend on whether the PT is first or second order as considered above (Sec. III B).

Imry and Wortis²⁷ predicted rounding of a first-order phase transition in the presence of quenched impurities or RF. This seems to explain the smearing of the discontinuities, if any, of θ versus H at H_{c1} (cf. Sec. III B). It is most effective at higher temperatures, where the presumed step heights gradually shrink. On the other hand, the $\Delta\theta$ effect upon field cycling increases very sensitively with decreasing temperature. This can be explained within the framework of the RFIM domain-state theory of Villain,³⁴ who predicts the domain sizes to scale as $R \propto T/h^2$, where T and h are the temperature and the random field, respectively. Assuming $\Delta\theta \propto R^{-1}$ (see Sec. IV A) one expects, indeed, the largest effects for $T \rightarrow 0$, where simultaneously also $h \propto M$ is maximized along the AF-SF phase boundary. Quantitatively the relation

$$\theta^2/\Delta\theta \propto h^2 R \propto T \quad (8)$$

should hold, as is indeed verified for $4 \text{ K} < T < 8 \text{ K}$ in Fig. 11. In this plot θ and $\Delta\theta$ refer to the bulk magnetization as measured at H_{c1} in the upward scan and to the excess magnetization found in the downward scan just below H_{c1} [Fig. 6(b)], respectively. For $T > 8 \text{ K}$, data are lacking owing to unmeasurably small $\Delta\theta$ values. Saturation of $\theta^2/\Delta\theta$ below $T^* \simeq 4 \text{ K}$ seems to indicate temperature independence of $R \propto \Delta\theta^{-1}$ for $T \rightarrow 0$. This is in qualitative agreement with recent theories³⁵ predicting constant minimum domain sizes in the low T limit. Our result, $T^* \simeq T_c/4$, is near to that given by Andelman and Joanny,³⁵ $T^* \simeq T_c/6$. To the best of our knowledge our data are the first to yield experimental evidence of this prediction. Very likely the concentrated spin systems used in this work are more appropriate towards these ends than the diluted AF, which are known to exhibit additional impurity pinning effects.^{19,25,35}

The high-field SF-PM transitions of $\text{Fe}_{0.73}\text{Co}_{0.27}\text{Cl}_2$ are very clearly rounded [Figs. 6(b) and 8], such that H_{c2} becomes ill-defined as discussed in Sec. III B. Similar rounding was found by Ito *et al.*²⁸ at the SF-PM transition of $\text{Fe}_{0.15}\text{Ni}_{0.85}\text{Cl}_2$. This mixture, as well, exhibits S_{\parallel}

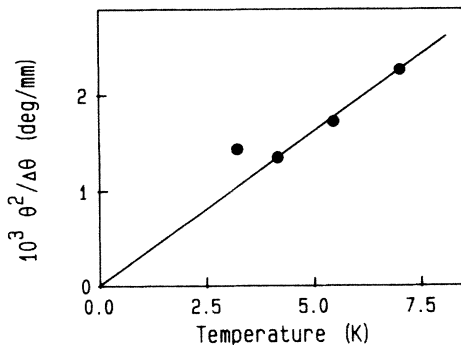


FIG. 11. $(\theta^2/\Delta\theta)$ vs T obtained on $\text{Fe}_{0.73}\text{Co}_{0.27}\text{Cl}_2$ upon isothermally cycling around the SF field H_{c1} [see Fig. 6(b) and text], best fitted to Eq. (8) within $4 \text{ K} < T < 8 \text{ K}$ (solid line).

ordering and has a near-tetracritical concentration ratio. RF effects were invoked to explain the rounding in that case. The experimental data, however, seem to be in conflict with two characteristic features of RF transitions: (i) FC usually affects merely the *critical* behavior and should, hence, produce rounding only in a very small range around the critical point, $|H/H_{c2} - 1| \lesssim 10^{-2}$, say; (ii) the FC induced domain state usually gives rise to enhanced magnetization [Figs. 3(b) and 4(b)] as discussed above. Assuming qualitatively the same results upon *isothermal* field cycles (field decreasing corresponding to FC), both characteristics are not met in the present case. Rounding occurs in the large range $|H/H_{c2} - 1| \lesssim 10^{-1}$ and hysteresis is lacking at *all* temperatures, $T \leq T_b = 14.8 \text{ K}$. We are, hence, rather inclined to attribute the observed rounding preponderantly to random *anisotropy* effects. These were treated in the case of thermally driven PT's at $H=0$ by Oku and Igarashi,³⁶ who predict increased smearing with increasing off-diagonal anisotropy energy. Diffuse phase transitions as a consequence of runaway fixed points are expected. Increasing roundings of the M versus H curves at H_{c2} of $\text{Fe}_{1-x}\text{Ni}_x\text{Cl}_2$ (Ref. 28) on decreasing x from 0.85 to 0.50 seem to support this view.

It should be noted that the random anisotropy mechanism does not primarily involve domain states, which were nevertheless evident from neutron scattering of the S_{\parallel} components in $\text{Fe}_{0.725}\text{Co}_{0.275}\text{Cl}_2$ by Wong and Cable.⁴ We believe this to be due to the now well-known¹³ three-fold intraplanar anisotropy, which becomes apparent in all phases involving finite S_{\perp} components. Very small domains are expected in the limit of vanishing internal strains. In our opinion there is no *a priori* evidence for the RF xy -model nature of the SF phase as proposed previously.⁴ In particular, RF effects can scarcely account for one yet unexplained feature of the SF phase, the decrease of χ_{\parallel} with increasing T [Fig. 6(b), 8]. Presumably, this is another effect of the off-diagonal spin interactions and may be connected with the unusual OAF ground state at $H=0$ and $T \lesssim 13 \text{ K}$.^{1,13} Note that the $H=0$ state is purely S_{\parallel} ordered at $T \gtrsim 13 \text{ K}$ (Fig. 1). Hence, random anisotropy effects are not expected to affect the AF-PM transition in the low- H limit, thus preserving its pure RFIM character [Fig. 5(b)].

V. SUMMARY

In accordance with the FA proposition (Ref. 6), the mixed uniaxial antiferromagnet $\text{Fe}_{1-x}\text{Co}_x\text{Cl}_2$, $x < x_c \sim 0.28$, exhibits similar RFIM properties as diluted systems like $\text{Fe}_{1-x}\text{Zn}_x\text{F}_2$ (Ref. 9) and $\text{Fe}_{1-x}\text{Mg}_x\text{Cl}_2$ (Ref. 18). This refers most notably to the now classical values of the exponents, $\phi \sim 1.40$ and $\tilde{\alpha} \sim 0$, obtained in the low-field limit. Owing to the similarity of the isotropic exchange constants of both FeCl_2 and CoCl_2 , the strength of the RF is fairly weak. This explains the large extension of the crossover range. It would be interesting to study related systems, involving larger differences of the J values. For example, in $\text{Fe}_{1-x}\text{Ni}_x\text{Cl}_2$ more important random field effects and a smaller crossover range are expected.³⁷

In $\text{Fe}_{1-x}\text{Co}_x\text{Cl}_2$ the attention is much more focused onto the spectacular effects due to "tuning" of the effective uniaxial anisotropy by admixture of Co^{2+} ions into FeCl_2 . In fields of the order of the anisotropy field the most remarkable issue is the x dependent crossover from metamagnetic to SF behavior due to the competition of the single-ion anisotropies involved. The concentration $x=0.20$ and 0.27 used in the present investigation, seem to bracket the crossover range predicted theoretically.⁷ Up to now no hint at the mixed phase diagram with SF behavior at low temperatures and spin-flip behavior at higher temperatures has been found.

Metastable domain states are evidenced by enhanced magnetization, ΔM , appear upon crossing the PM-AF and the SF-AF phase boundaries from high temperatures ($H=\text{const}$) or high fields ($T=\text{const}$), respectively. Very probably, ΔM is concentrated on the induced domain walls, which are believed to be particularly Co^{2+} rich.

Domain size R versus T predictions³⁵ could be confirmed indirectly for the first time.

The marked smearing of the SF-PM phase transition hints at random anisotropy effects, which seem to hamper the oblique spin ordering¹³ in the SF phase. We believe that random-field effects are of minor importance at this phase boundary. The domain state found in the SF phase⁴ may solely be explained by magneto-elastic effects, which arise in the space group $3\bar{R}m$ whenever oblique spin ordering occurs.¹³

ACKNOWLEDGMENTS

Thanks are due to H. Junge for help with the crystal growth and to U. A. Leitão for discussions. This work was supported by the Deutsche Forschungsgemeinschaft (Bonn, Germany) within the framework of "Sonderforschungsbereich 166."

- ¹P. Z. Wong, P. M. Horn, R. J. Birgeneau, and G. Shirane, *Phys. Rev. B* **27**, 428 (1983).
²P. Z. Wong, *Phys. Rev. B* **34**, 1864 (1986).
³P. Z. Wong and J. W. Cable, *Solid State Commun.* **51**, 545 (1984).
⁴P. Z. Wong and J. W. Cable, *Phys. Rev. B* **30**, 485 (1984).
⁵T. E. Wood and P. Day, *J. Magn. Magn. Mater.* **15-18**, 782 (1980).
⁶S. Fishman and A. Aharony, *J. Phys. C* **12**, L729 (1979).
⁷S. Galam and A. Aharony, *J. Phys. C* **13**, 1065 (1980).
⁸Y. Imry and S.-k. Ma, *Phys. Rev. Lett.* **35**, 1399 (1975).
⁹V. Jaccarino, in *Condensed Matter Physics—The Theodore D. Holstein Symposium*, edited by R. L. Orbach (Springer, New York, 1987), p. 47.
¹⁰A. Aharony, *Europhys. Lett.* **1**, 617 (1986).
¹¹L. C. Le Guillou and J. Zinn-Justin, *Phys. Rev. B* **21**, 3976 (1980).
¹²G. Jug, *Phys. Rev. B* **27**, 609 (1983).
¹³W. Nitsche and W. Kleemann, *J. Magn. Magn. Mater.* **54-57**, 37 (1986); *Phys. Rev. B* **36**, 8587 (1987).
¹⁴W. Kleemann, A. R. King, and V. Jaccarino, *Phys. Rev. B* **34**, 479 (1986).
¹⁵J. A. Griffin, S. E. Schnatterly, Y. Farge, M. Régis, and M. P. Fontana, *Phys. Rev. B* **10**, 1960 (1974).
¹⁶Y. Shapira, *J. Appl. Phys.* **57**, 3268 (1985).
¹⁷J. Villain, *Phys. Rev. Lett.* **52**, 1543 (1984).
¹⁸U. A. Leitão and W. Kleemann, *Phys. Rev. B* **35**, 8696 (1987).
¹⁹C. M. Soukoulis, G. S. Grest, C. Ro, and K. Levin, *J. Appl. Phys.* **57**, 3300 (1985); G. S. Grest, C. M. Soukoulis, and K. Levin, *Phys. Rev. B* **33**, 7659 (1986).
²⁰A. R. King, V. Jaccarino, T. Sakakibara, M. Motokawa, and M. Date, *J. Magn. Magn. Mater.* **31-34**, 1119 (1983).
²¹F. A. Modine and R. W. Major, *Appl. Opt.* **14**, 761 (1975).
²²F. Seitz, T. E. Wood, and P. Day, *Z. Naturforsch.* **35a**, 1013 (1980).
²³J. Pommier, J. Ferré, and S. Senoussi, *J. Phys. C* **17**, 5621 (1984).
²⁴J. F. Dillon, Jr., E. Yi Chen, and H. J. Guggenheim, *Phys. Rev. B* **18**, 377 (1978).
²⁵H. Yoshizawa and D. P. Belanger, *Phys. Rev. B* **30**, 5220 (1984).
²⁶L. J. de Jongh and A. R. Miedema, *Adv. Phys.* **23**, 1 (1974).
²⁷Y. Imry and M. Wortis, *Phys. Rev. B* **19**, 3580 (1979).
²⁸A. Ito, E. Torikai, M. Kitazawa, T. Tamaki, T. Goto, T. Sakakibara, S. Todo, and I. Oguro, *J. Magn. Magn. Mater.* **54-57**, 39 (1986).
²⁹H. Rohrer, *J. Appl. Phys.* **52**, 1708 (1981).
³⁰W. J. Tabor and F. S. Chen, *J. Appl. Phys.* **40**, 2760 (1969).
³¹D. Mukamel, *Phys. Rev. Lett.* **46**, 845 (1981).
³²D. P. Belanger, A. R. King, and V. Jaccarino, *Phys. Rev. B* **34**, 452 (1986).
³³D. P. Belanger, A. R. King, I. B. Ferreira, and V. Jaccarino, *Phys. Rev. B* **37**, 226 (1988).
³⁴J. Villain, in *Scaling Phenomena in Disordered Systems*, edited by R. Pynn and A. Skjeltorp (Plenum, New York, 1985), p. 423.
³⁵R. Bruinsma and F. Aeppli, *Phys. Rev. Lett.* **52**, 1547 (1984); D. Andelman and J. F. Joanny, *Phys. Rev. B* **32**, 4818 (1985); T. Nattermann, *Phys. Status Solidi B* **129**, 153 (1985).
³⁶M. Oku and H. Igarashi, *Prog. Theor. Phys.* **70**, 1493 (1983).
³⁷P. Z. Wong, J. W. Cable, and P. Dimon, *J. Appl. Phys.* **55**, 2377 (1984).